Geophysical Research Letters

RESEARCH LETTER
10.1029/2019GL083953

Bathymetry of Southeast Greenland From Oceans Melting Greenland (OMG) Data

Lu An[1], Eric Rignot[1,2,3], Nolwenn Chauche[4], David M. Holland[5,6], Denise Holland[5,6], Martin Jakobsson[7], Emily Kane[1], Michael Wood[1], Ingo Klaucke[8], Mathieu Morlighem[1], Isabella Velicogna[1,2], Wilhelm Weinrebe[8], and Josh K. Willis[2]

[1]Department of Earth System Science, University of California, Irvine, CA, USA, [2]Jet Propulsion Laboratory, California Institute of Technology, Pasadena, CA, USA, [3]Department of Civil and Environmental Engineering, University of California, Irvine, CA, USA, [4]Access Arctic, Le Vieux Marigny, France, [5]Courant Institute of Mathematical Sciences, New York Univerisity, NY, USA, [6]Center for Global Sea Level Change, New York University Abu Dhabi, Abu Dhabi, United Arab Emirates, [7]Department of Geological Sciences, Stockholm University, Stockholm, Sweden, [8]GEOMAR Helmholtz Centre for Ocean Research Kiel, Kiel, Germany

Abstract Southeast Greenland has been a major participant in the ice sheet mass loss over the last several decades. Interpreting the evolution of glacier fronts requires information about their depth below sea level and ocean thermal forcing, which are incompletely known in the region. Here, we combine airborne gravity and multibeam echo sounding data from the National Aeronautics and Space Administration's Oceans Melting Greenland (OMG) mission with ocean probe and fishing boat depth data to reconstruct the bathymetry extending from the glacier margins to the edges of the continental shelf. We perform a three-dimensional inversion of the gravity data over water and merge the solution with a mass conservation reconstruction of bed topography over land. In contrast with other parts of Greenland, we find few deep troughs connecting the glaciers to the sources of warm Atlantic Water, amidst a relatively uniform, shallow (350 m) continental shelf. The deep channels include the Kangerlugssuaq, Sermilik, Gyldenløve, and Tingmiarmiut Troughs.

Key Points:
- A multisensor approach resolves the bathymetry on the continental shelf and glacial fjords of southeast Greenland
- Few deep or complex networks of troughs connect the glaciers to the sources of warm Atlantic Water; that is, access to ocean heat is limited
- The new bathymetry helps interpret the past and recent evolution of southeast Greenland glaciers and contribution to sea level rise

Supporting Information:
- Supporting Information S1

Correspondence to:
L. An,
an.lu@uci.edu

Citation:
An, L., Rignot, E., Chauche, N., Holland, D., Holland, D., Jakobsson, M. et al. (2019). Bathymetry of southeast Greenland from oceans melting Greenland (OMG) data. *Geophysical Research Letters*, *46*, 11,197–11,205. https://doi.org/10.1029/2019GL083953

Received 10 JUN 2019
Accepted 12 AUG 2019
Accepted article online 21 AUG 2019
Published online 21 OCT 2019

1. Introduction

The mass loss of the Greenland Ice Sheet increased from 41±17 Gt/year in 1990–2000 to 286±20 Gt/year in 2010–2018 (Mouginot et al., 2019). During the period 1972–2018, glaciers from southeast Greenland contributed the second largest mass loss to sea level rise (3.0±0.3 mm) behind northwest Greenland (4.4±0.2 mm). Southeast Greenland produces the largest discharge of ice (136±6 Gt/year) in Greenland versus the other seven regions in 1972–1980, and the discharge increased into 160±2 Gt/year in 2010–2018 (Mouginot et al., 2019). While the rapid increase in ice discharge of Helheim Gletscher in 2000–2004 has been well documented (Howat et al., 2005, 2011), other glaciers including Køge Bugt, Umiivik Fjord, A.P. Bernstoff, Tingmiarmiut Fjord, and Anorituup Kangerlua are now recognized to have been major participants in the mass loss from the region (Mouginot et al., 2019). These marine-terminating glaciers interact vigorously with the surrounding ocean waters which are among the warmest in Greenland because they originate directly from the Gulf Stream (Straneo et al., 2012). A leading hypothesis for the glacier evolution in southeast Greenland has been that the intrusion of warm Atlantic Water (AW) in the fjords increased in the 1990s, melted the glacier fronts, destabilized them, and increased mass discharge (Christoffersen et al., 2011; Holland et al., 2008; Howat et al., 2008; Howat & Eddy, 2011; Murray et al., 2010). Until recently, however, few ocean measurements have been available to document water temperature in the fjords (Murray et al., 2010), which makes it difficult to interpret the observed glacier changes and how they varied from one fjord to the next. Similarly, the bathymetry of the fjords and the continental shelf has been known incompletely in this region. For example, the International Bathymetric Chart of the Arctic Ocean version 3.0 (IBCAO Ver. 3.0) does not include quality data in the fjords (Jakobsson et al., 2012). The lack of bathymetry, with a few exceptions, makes it difficult to understand or model how warm, salty, subsurface (depth >350 m) AW may intrude on the continental shelf, into the glacial fjords and then reach the glaciers.

In 2015, the National Aeronautics and Space Administration launched the Oceans Melting Greenland (OMG) mission (Fenty et al., 2016) to collect a suite of data, including multibeam echo sounding (MBES), airborne gravity, airborne surface topography, and ocean physical properties from Airborne eXpendable Conductivity, Temperature and Depth (AXCTD) probes and more conventional ship-based CTDs (An

et al., 2019; Wood et al., 2018). These data have been instrumental in constraining a reconstruction of glacier thickness and bed elevation on land ice from mass conservation, BedMachine v3 (BMv3; Morlighem et al., 2017). The results helped significantly improve our knowledge of glacier fluxes in southeast Greenland (Millan et al., 2018; Mouginot et al., 2019). The revised discharge estimates were 39% higher than prior estimates due to the underestimation of bed elevation beneath many fast-flowing outlet glaciers. The fjord bathymetry revealed which fjords are protected from AW by sills and which were not (Batchelor et al., 2019), where glacier fronts stand with respect to the depth of warm AW, and how this position has evolved in the last few decades of retreat.

Our knowledge of the bathymetry on the continental shelf has remained incomplete, however, which makes it difficult to relate the changes observed in glacial fjords with changes in the outer ocean, for example, in the Irminger Current. Warm, salty, subsurface AW tends to follow preferential troughs across the continental shelf that have been carved by glaciers in prior times, but not knowing if these troughs and additional channels exist and where they are located makes it challenging to understand glacier evolution.

In this study, we present a three-dimensional inversion of the OMG gravity data along coastal southeast Greenland constrained by independent observations, including OMG MBES data and single-beam data available since IBCAO Ver. 3.0. We employ these observations to reconstruct the bathymetry from the glacier margins to the edge of the continental shelf. We describe the data and methods, the quality of the results, and their implications for understanding the glacier evolution of southeast Greenland.

2. Data and Methods

2.1. Airborne Gravity

We collected airborne gravity data over Helheim Gletscher using Sander Geophysics Limited Airborne Inertially Referenced Gravimeter (AIRGrav) deployed on a Eurocopter AS355 F2 operated by HeliGreenland from 16 to 27 August 2012. We refer to the gravity data as the Gordon and Betty Moore Foundation gravity data. AIRGrav operated with a line spacing of 500 m, at a target speed of 50 knots (1 knot = 0.51 m/s), with 80-m clearance above the ground. Accelerometer data were recorded at 128 Hz and later decimated to 2 Hz in processing. The instrument noise level is better than 0.5 mGal with a half-sine wave ground resolution of 1.8 to 2 km. The helicopter was instrumented with NovAtel OEMV-V3 GPS receivers combined with a GPS reference station using a Novatel DL-4Pplus integrated GPS and data logger. Sander Geophysics Limited's proprietary software was used for data processing. GPS data were recorded at 10 Hz. The calculated gravity was corrected for Eötvös effect, theoretical gravity, free air correction, static correction, and level correction. A 20-s half-wavelength filter was used to reduce data noise. The data were filtered with a 750-m half-wavelength low-pass filter. A 28-s half-wavelength filter was used for intersection statistics.

In 2016, OMG collected airborne gravity data over the ocean surface using the AIRGrav deployed on a Cessna Grand Caravans 208B from 28 May to 30 June 2016, from the airport of Kulusuk. The survey speed was 110 knots with a sea level clearance of 150 m. The gravity data were acquired over open ocean for a combined 33,232 km of the flight lines. Gravity lines flown closest to shore were flown at 2-km spacing versus 4 km farther offshore (Figure 1). Onboard receivers were NovAtel OEMV-3; the reference station used a NovAtel OEM4 GPS receiver. The outer lines were gridded at 1-km grid cell size; the inner lines were at 500 m. The data were filtered with a 1-km half-wavelength filter. The root-mean-square crossover error is 1.5 mGal.

2.2. MBES, CTD, and AXCTD Data

MBES data were collected by Terrasond Ltd. from 9 September to 7 October 2016, onboard the M/V Neptune for a total of 3,717 linear nautical miles (6,884 km) using a hull-mounted Reson 8160 sonar, 50-kHz, multibeam echo sounder. A complimentary survey was conducted in August 2018 onboard the S/Y Ivilia operated by Arctic Access using Helmholtz Centre for Ocean Research Kiel (GEOMAR) SeaBeam 1050 multibeam echo sounders. Calibrations of sound speed in water for the multibeam echo sounders were performed using CTD data collected at regular intervals (An et al., 2018). An AML Oceanographic Minos X CTD was used under thick brash/sea ice conditions. In ice-free ocean waters, a Valeport Rapid CTD was deployed. The Caris HIPS software was used to process the MBES data. The data are provided in 25- and 50-m gridded format.

AXCTD data were collected on a Grumman Gulfstream III aircraft in September/October 2016, C-130 Hercules in October 2017, and a Basler DC-3 Turbo Prop in August/September 2018. These expendable

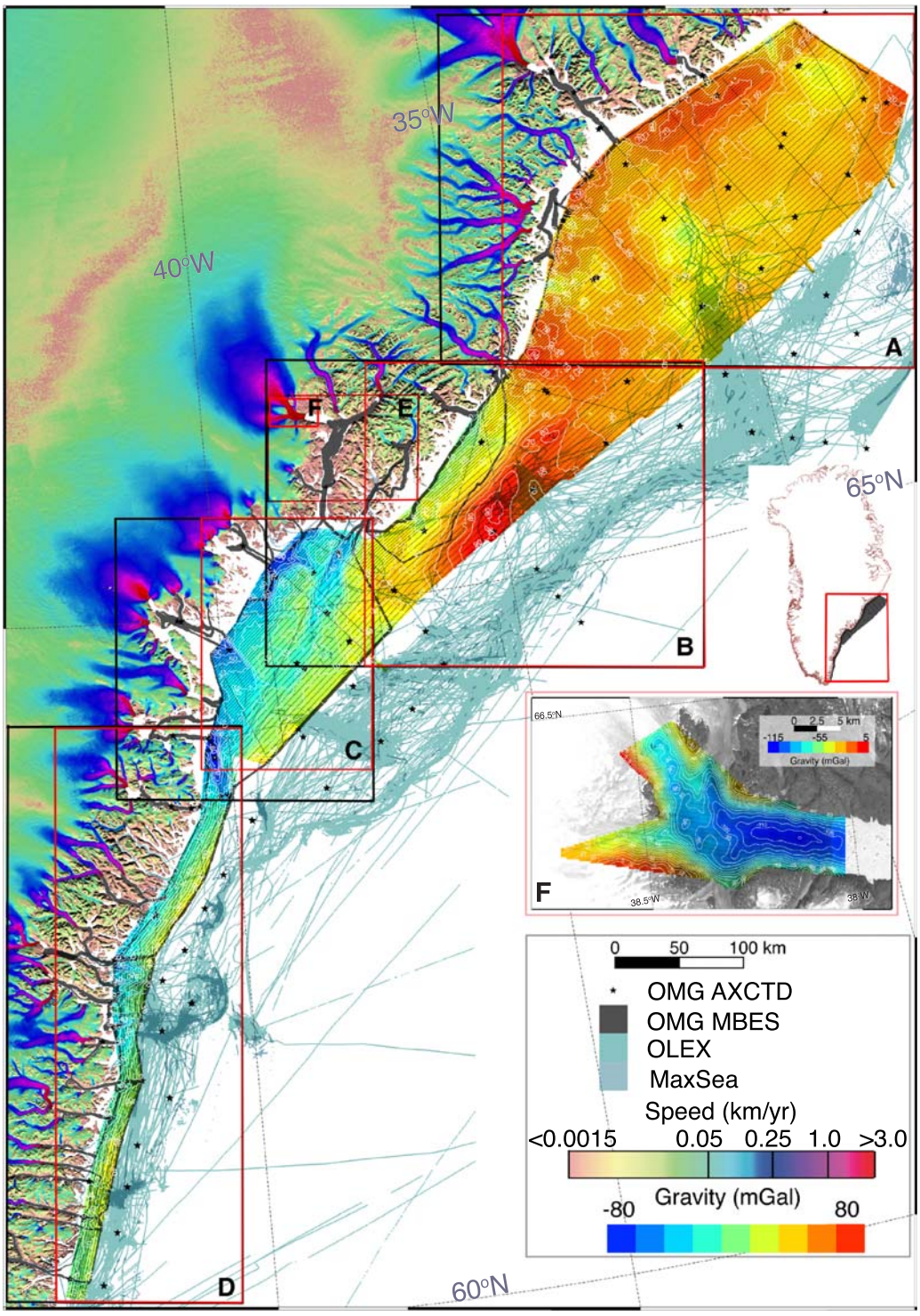

Figure 1. Survey lines (black thin line) of OMG airborne gravity in southeast Greenland, with AXCTD from 2016 to 2018 (black stars), MBES data (dark gray), Olex (dark green), and MaxSea (pale green) overlaid on a map of ice speed color coded on a logarithmic scale. Four blocks A–D (red box) divide the domain. Block E is Sermilik Fjord. Block F is Gordon and Betty Moore Foundation gravity survey lines on Helheim Gletscher, color coded separately. Red boxes show the gravity inversion domains. Black boxes represent the subregions shown in remaining figures. Inset shows the location of the surveyed domain in Greenland. Free-air gravity anomalies in milligal (1 mGal = 10^{-5} m/s^2) are color coded from blue (−80 mGal) to red (+80 mGal) with 10-mGal white contours for OMG gravity. AXCTD = Airborne eXpendable Conductivity, Temperature and Depth; OMG = Ocean Melting Greenland; MBES = multibeam echo sounding.

instruments are launched from an aircraft, fall under a small parachute and float on the surface after impact. The floating portion then releases a probe, which sinks to a depth of up to 1,000 m. The probe is connected to the float by a thin wire which unspools as the probe sinks, measuring temperature and conductivity as a function of time. This information is sent by radio to the aircraft, where it is used to compute temperature and salinity as a function of depth. As each AXCTD collects data until it hits the seafloor, it provides information about seafloor depth in addition to temperature and salinity. During the ship survey, more traditional lowered CTD data were collected. Some of CTD casts reached the seafloor and are therefore used to constrain seafloor depth. The seafloor depth was also measured from eXpendable Current profiler (XCP) and Conductivity Temperature Depth (XCTD) probes dropped from helicopters between 2009 and 2018 in Helheim Fjord, which we use to constrain the inversion (Figure 1 and supporting information Figure S1). We have a total of 12 XCTDs in the proximity of Helheim Gletscher.

Finally, we use available single-beam data from the Olex seabed mapping system (www.olex.no) and crowd-sourced data from fishing and recreational vessels (MaxSea; Figure 1). The data were filtered using a block median filter and thresholds to eliminate numerous bad picks and reduce crossover errors.

2.3. Gravity Inversion

The gravity inversion is performed using Geosoft GM-SYS 3-D which implements the method of Parker (1972) that iteratively minimizes the misfit between calculated and observed gravity. We divide the survey domain into four parts A–D to ease the computation (Figure 1). The model domain is represented as three horizontal layers: (1) a solid ice layer with a density of 0.917 g/cm^3, (2) an ocean water layer with density 1.028 g/cm^3, and (3) a rock layer with density 2.67 g/cm^3. In a prior study, we showed that the three-layer model provided superior performance compared to a four-layer model, that is, that would include rock density as a variable or the depth of fresh sediments (An et al., 2018). A forward model of gravity is calculated using BMv3 (Morlighem et al., 2017) as the initial bed solution (Figure S2a). We calculate the direct current (DC) shift or difference between modeled and observed gravity at locations where the seafloor depth is known from MBES data, single-beam soundings, CTD, or AXCTD (Figure S2b). We note that parts A–D are constrained by observations of seafloor depth around their entire periphery. The DC shift exhibits spatial variations that reflect variations in the unknown underlying geology. We interpolate the DC shift onto a regular grid using a minimum curvature algorithm (Smith & Wessel, 1990; Figure S2c). We then correct the observed gravity with the interpolated DC shift and use it as input to the inversion model to account for the original model bias. Subsequently, we fill in observational gaps with the resulting, regionally corrected modeled data (Figure S2d). This process minimizes the impact of data gaps on the inversion at the edges of the survey. We allow a 1,500-m-(horizontal)wide transition between observation and model to enable a smooth transition that preserves the observations. The inversion minimizes the misfit between observed and modeled gravity. Grid spacing is 500 m.

For Helheim Gletscher, we perform a similar inversion with gravity data gridded at 500 m. Constraints for the inversion are BMv3 on land, 2018 MBES data in the fjord, and seafloor depth from XCP and XCTD from various years (Figure S1a). Several iterations were performed to obtain a smooth transition in bed topography between land and fjord bed elevation, preserving mass conservation on land and consistent with the gravity data at sea. A data gap remains between the airborne gravity and MBES data that is only filled with discrete XCP and XCTD data.

We generate an error map for the bathymetry product (Figure S3). The uncertainty is 1–2 m with MBES data, 10 m with Olex and MaxSea, and 100 m for IBCAO Ver. 3.0. For gravity, we translate the misfit into an error in bed elevation using a conversion of 5 mGal per 100 m of water obtained from forward model simulations (An et al., 2019). We find an error of $\pm$60 m consistent with the error derived from the gravity misfit.

3. Results

3.1. Helheim Gletscher

The observed gravity anomalies in the Helheim inversion domain vary from $-$115 mGal in the fjord to +5 mGal in the surrounding mountain peaks, with negative values in the ocean and the main glacier trunk (Figure 1, Box F). Bed elevation is positively correlated with gravity anomaly, as expected for nearly uniform geology (Figure S1b). The gravity inversion yields a fjord that is U shaped, consistently deep from the glacier front to the entrance of Sermilik fjord (Figure 2). We find no sill near the front of Helheim. We have,

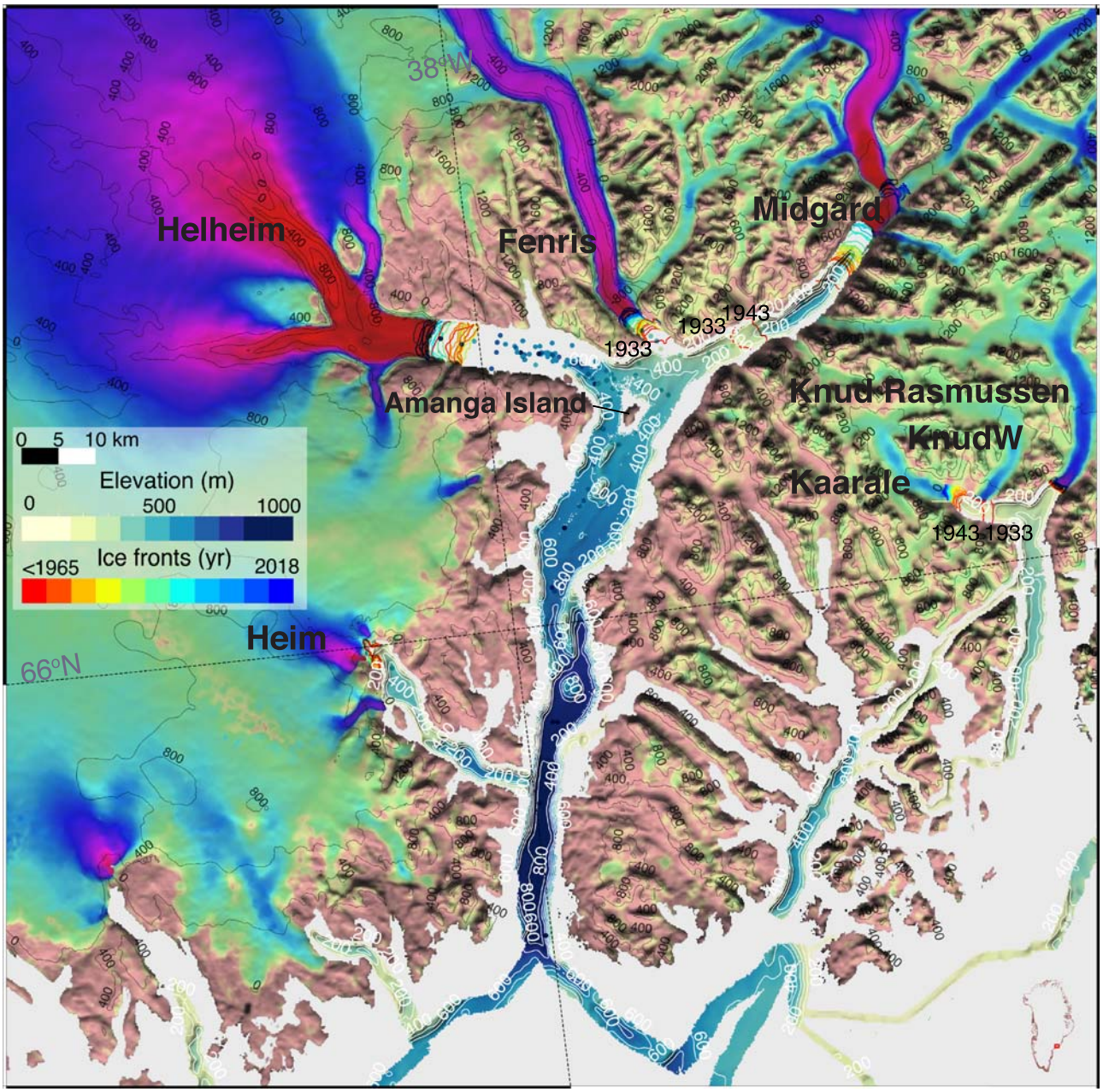

Figure 2. Bed topography and bathymetry near Sermilik Fjord, southeast Greenland, with Helheim and Midgård glaciers. Bed contours are white (100 m) with labels every 200 m. Historical ice front locations from 1933 to present are color coded by date with 1933 and 1943 locations labeled. Ice speed on land is color coded on a logarithmic scale from brown (no motion) to yellow, green, blue, and red (fastest motion), overlaid on bed contours. Other major glaciers include Heim, Fenris, Kaarale, and Kund Rasmussen.

however, a data gap only partially filled with discrete seafloor depth. Comparing the 2018 MBES data in Sermilik fjord with a bathymetry assembled from single-beam data (Morlighem et al., 2017), we find a reasonable agreement between single-beam and multibeam data within errors (Figure S4). Sermilik fjord is 800 m below sea level (bsl) south of 66°N and relatively flat, which is indicative of high sediment deposition, and 600 mbsl north of 66°N. The fjord remains consistently deep toward Helheim Gletscher. In contrast, we find a 200-m-deep sill at the entrance of Midgård fjord, which coincides with the ice front location in the year 1933. Midgård fjord is shallow at its entrance and deepens slowly to 400–500 mbsl until the limit of our survey, which coincides with the ice front location in the 1980s.

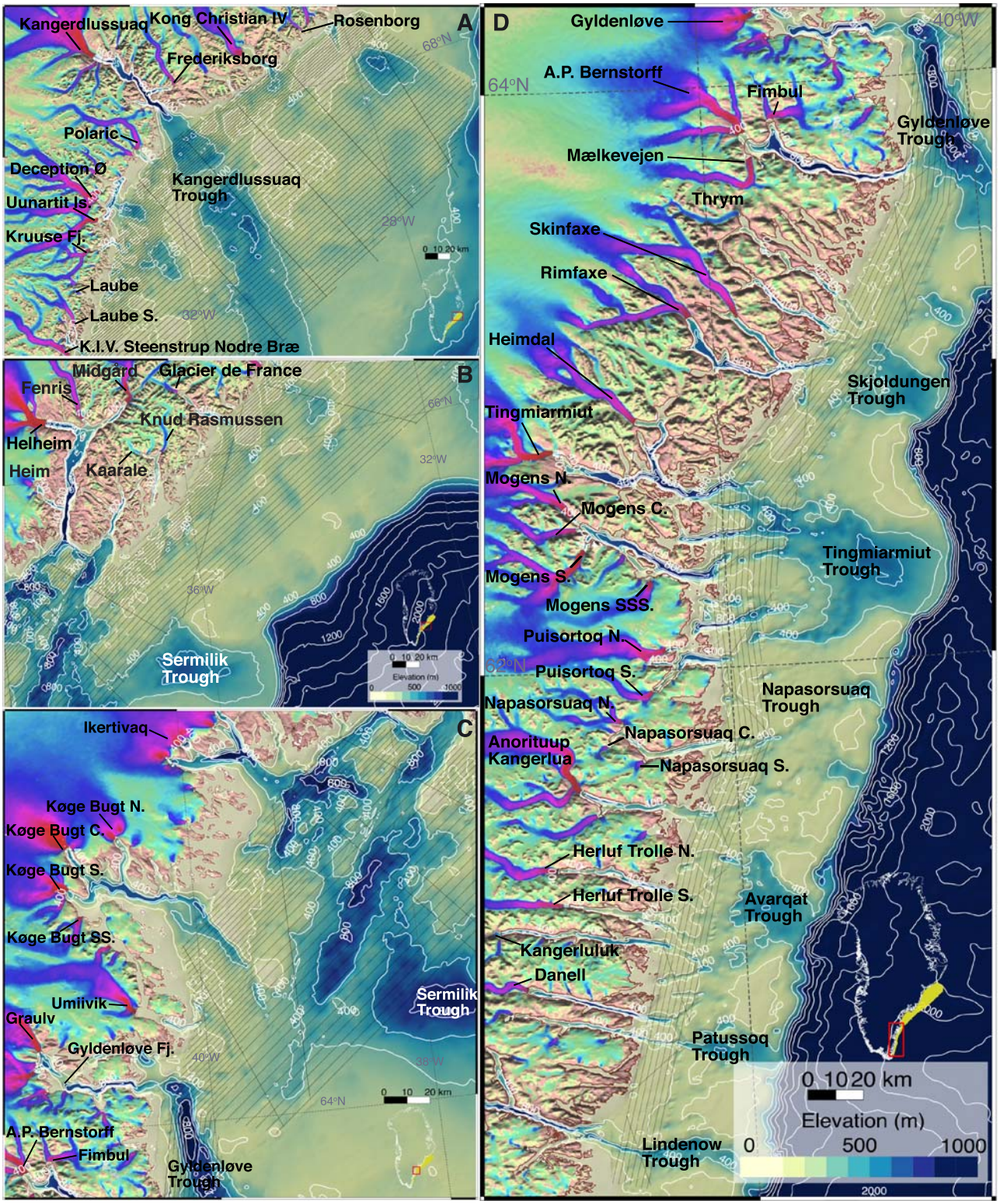

Figure 3. Bathymetry in southeast Greenland, with panels corresponding to subregions A–D of the inversion domain (Figure 1). Bed elevation is color coded from white (0 m) to blue (1,000 m) above mean sea level with 200-m contours and labels every 400 m. The ice-ocean boundary is brown. Major glaciers and troughs on the seafloor are named. Black thin lines are survey lines from gravity.

3.2. Southeast Coast

The observed gravity anomalies within the survey area vary from −94 mGal in the troughs connected the glacier fjords to +92 mGal on the continental shelf (Figure 1). The inferred bed elevation is positively correlated with gravity anomaly (Figure 3). The major glacier in Block A is Kangerdlussuaq, with the Kangerdlussuaq Trough (KT) which extends to the edge of the continental shelf. We find a previously unknown narrowing of the KT channel 36 km outside of the main fjord which may play a role in controlling the access of warm water to the glacial fjord. The depth of the seafloor in front of the K.I.V. Steenstrup Nodre Bræ and Laube Glacier is 100 m shallower than in previous maps. Most of the continental shelf in the region is rather uniform and shallow in depth. We find no deep trough in front of the complex and active glacier system of Deception Ø, Uunartit Island, and Kruuse Fjord.

The bathymetry in Block B is relatively uniform (Figure 3b), with few places exceeding 400 m in depth. The average depth of the continental shelf is about 350 m. We find a 50-m-deep sill at the entrance of the fjord that hosts Glacier de France and no deep trough in front of Kund Rasmussen. The bathymetry outside Sermilik fjord is more complex, with two deep channels (500–700 mbsl) bifurcating in southeasterly and southwesterly directions (Figure 3b) and separated by a shallow area less than 200 mbsl. These channels do not cross the continental shelf but narrow down to 300 mbsl farther south (Figure 3c) to coalesce into the 800-m-deep Sermilik Trough (ST). The southwesterly branch connects with a trough emerging from Ikertivaq which has a sill depth of 400 mbsl (Figure 3c). Conversely, the 600-m-deep glacial fjord Køge Bugt connects to ST after shallowing to 300 mbsl (Figure 3c). We have an incomplete bathymetry for Umiivik which starts with a 400-m-deep fjord that shallows on the continental shelf.

At the southern end of Block C, we find the 600- to 1,000-mbsl Gyldenløve Trough (GT) offshore Gyldenløve fjord which hosts several glaciers, for example, Graulv glacier. The fjord is 800 m deep, shallowing to 400 mbsl at its entrance before overdeepening to 1,000 mbsl about 30 km offshore. GT is the deepest and largest trough in Southern Greenland after ST, hence revealing a prominent past glacial system at that location.

In Block D, we find that the Bernstorffs fjord, which hosts A.P. Bernstroff, Fimbul, Mælkevejen, and others, connects with GT via a shallowing at 300 mbsl (Figure 3d). Farther south, the Skjoldungen Trough (SKT) is more than 400 mbsl and connects with Rimfaxe and Skimfaxe glaciers via a 300-m deep narrowing at the fjord entrance. The next prominent system farther south is the Tingmiarmiut Trough, which connects with Heimdal, Tingmiarmiut, Mogens, Heinesen N, and Puisortoq. Most of those fjords are 600–800 mbsl, but they shoal to 300–400 mbsl at the fjord entrance. Farther south, the signature of glacial fjords on the continental shelf is weaker. The Napasorsua Trough is not a major trough, and the Avarqat Trough is not strongly connected to glacial fjords. The Patussoq Trough and the Lindenow Trough connect to rather narrow glacial fjords (a few kilometers) at the southern end of the domain at 400 mbsl.

4. Discussion

In Sermilik fjord, the MBES data reduce prior uncertainty in bed mapping by 50 m. Following an entrance deeper than 800 m, the middle of the fjord raises to 600 m, with a relatively flat bottom (Figures 2 and S4). The fjord narrows and shallows to the east, toward Midgård Glacier, but not to the west toward Helheim. At the location of the 1930 ice front of Midgård, we find a 200-m sill which must have stabilized the ice front prior to the 1930s and must now limit the access of AW, which is mostly below 300-m depth. Beyond the sill, the bed deepens to 450-m until the edge of the survey. This retrograde bed explains the rapid and sustained 18-km glacier retreat from the 1930s until the 1980s, the most extensive retreat during this period of any glacier in Greenland. In contrast, Sermilik fjord remains more than 500 m deep, but we find a shoaling around Amanga island to about 400 m (Figure 2). This bathymetric rise must contribute to the year-round presence of ice melange in Helheim Fjord. We find no sill west of the island toward Helheim. The largest obstacles to the intrusion of AW are therefore the shoaling around Amanga Island and on the outer shelf east of ST.

North of Sermilik fjord, our data confirm the general shape of the 40-km wide, 500-m-deep KT with a narrow passage at 400 mbsl about 36 km from the mouth of the fjord that must control the amount of AW reaching the glacier. We have few single-beam data in that precise sector to evaluate the inversion. In Block B, the continental shelf is relatively shallow and uniform. If troughs are present, they are not deep and wide. In Block C, we find the termination of Sermilik fjord and the presence of a narrowing at the entry of Ikertivaq. Similarly, the deep fjord of Køge Bugt does not connect to the edge of the shelf, hence protecting the

glaciers from the warmest waters off the continental shelf. The deepest trough, GT, is interrupted by several sills which probably partially block the access of the warmest AW to the glaciers. The next troughs farther south are broader on the edge of the shelf but narrow and shallow at the mouth of the fjords and hence are not highly conducive to transport of ocean heat. We map bathymetry at a 2-km spacing, with an accuracy of ±60 m. While this measurement performance is less than that achievable with MBES (25-m spacing, 1–2 m vertical for the OMG bathymetry data), the gravity data are critical to fill data gaps. The differences between IBCAO Ver. 3.0 and the OMG-derived gravity inversion are significant (Figures 3 and S5). In IBCAO Ver. 3.0, large expenses of nearly flat, shallow seafloor on the continental shelf make it impossible for subsurface AW to reach the glaciers in a numerical model of ocean circulation. If our bathymetry is correct, the access of AW in the fjords of southeast Greenland is broadly limited to the depth of about 300–350 mbsl on the continental shelf, in contrast with fjords that exhibit depths in the range of 400 to 600 m or deeper.

Overall, the geomorphology of southeast Greenland glaciers is different from west Greenland. The southeast glaciers flow down long, narrow valleys amidst an alpine landscape. The transition in elevation from land to sea is abrupt. The glacier fjords are deep, but the channels become shallower and broader at the mouth of the fjords and junction with the continental shelf, indicating that former ice streams did not erode the continental shelf as effectively, except perhaps for GT and Tingmiarmiut Trough. This configuration is consistent with glaciers extending to the edge of the continental shelf over this sector at the LGM (Batchelor et al., 2019; Dowdeswell et al., 2010). Driven by the intrusion of warm and salty water from the Irminger Current (Dyke et al., 2018), this region began the deglacial retreat around 17 ka (Jennings et al., 2006). The analysis of the two warming events in the 1930s and 2000s by Bjørk et al. (2012) showed that glaciers in the entire southeast region, no matter their type, size, or terminal environment, reacted simultaneously to the change in the ocean environment. After the early 2000s speedup of southeast glaciers, a widespread and synchronous slowdown took place. We find the synchronous retreat to be consistent with the presence of blocking sills at about the same depth (350 m) along the coast. We also note that this shallow depth (350 m) is above most of the warm waters in southeast Greenland, that is, the blocking sills must also have a significant impact on the amount of ocean heat that can reach the fjords. Numerical modeling of the ocean heat transport from the continental shelf to the glaciers will be critical to fully quantify the effectiveness of ocean heat transport from off the shelf, to the shelf, and into the fjords in that region.

The widths and depths of the fjords in southeast Greenland are correlated with the drainage basin areas of the glaciers. In Block D, the inner fjord and midfjord moraines suggest that the glaciers were either on a still stand or readvanced during the last deglaciation (Batchelor et al., 2019). Narrower and shallower fjords tend to stabilize the glaciers by increasing basal and lateral drag. Narrow fjords also reduce mass flow across the grounding zone, the rate of iceberg calving, and the intrusion of warm AW to the glaciers (Porter et al., 2014; Rignot et al., 2016).

5. Conclusions

In this study, we present a novel three-dimensional inversion of the OMG gravity data collected in southeast Greenland to infer the bathymetry of the continental shelf from its eastern edge to the entry of glacial fjords. The new bathymetric solution will be included in BedMachine v4 and is available at the OMG website (omg.jpl.nasa.gov). The first complete description of the bathymetry around southeast Greenland confirms the presence of a relatively broad and shallow continental shelf in the north with few deep troughs and connections with the warmest ocean waters, and a narrow but still shallow continental shelf to the south, with few incised troughs that often include a narrowing and shoaling close to the mouth of the glacial fjords. The fact that the depth of the seafloor is close to the depth of the warmest waters (about 350 m) makes it imperative to employ precise ocean numerical models to fully quantify ocean heat transport in that sector. The new bathymetry data will be transformative of modeling activities in the region and turn the quantification of the impact of ocean heat on past, present, and future glacier evolution in southeast Greenland.

Acknowledgments
This work was performed in the Department of Earth System Science, University of California, Irvine, and at Caltech's Jet Propulsion Laboratory under a contract with the National Aeronautics and Space Administration. We thank the technical personnel from Sander Geophysics Ltd and its aircraft crew from conducting the gravity survey of Greenland in the year 2016, the crew of TerraSond Ltd, M/V Cape Race, and Access Arctic for conducting the bathymetric surveys of 2016 and 2018.

References

An, L., Rignot, E., Millan, R., Tinto, K., & Willis, J. (2019). Bathymetry of Northwest Greenland using "Ocean Melting Greenland" (OMG) high-resolution airborne gravity and other data. *Remote Sensing*, *11*(2), 131.

An, L., Rignot, E., Mouginot, J., & Millan, R. (2018). A century of stability of Avannarleq and Kujalleq Glaciers, West Greenland, explained using high-resolution airborne gravity and other data. *Geophysical Research Letters*, *45*, 3156–3163. https://doi.org/10.1002/2018GL077204

Batchelor, C. L., Dowdeswell, J. A., Rignot, E., & Millan, R. (2019). Submarine moraines in Southeast Greenland fjords reveal contrasting outlet-glacier behaviour since the Last Glacial Maximum. *Geophysical Research Letters*, *46*, 3279–3286. https://doi.org/10.1029/2019GL082556

Bjørk, A. A., Kjær, K. H., Korsgaard, N. J., Khan, S. A., Kjeldsen, K. K., Andresen, C. S., et al. (2012). An aerial view of 80 years of climate-related glacier fluctuations in southeast Greenland. *Nature Geoscience*, *5*, 427–432. https://doi.org/10.1038/NGEO1481

Christoffersen, P., Mugford, R. I., Heywood, K. J., Joughin, I., Dowdeswell, J. A., Syvitski, J. P. M., et al. (2011). Warming of waters in an East Greenland fjord prior to glacier retreat: Mechanisms and connection to large-scale atmospheric conditions. *Cryosphere*, *5*(3), 701–714.

Dowdeswell, J. A., Evans, J., & ÓCofaigh, C. (2010). Submarine landforms and shallow acoustic stratigraphy of a 400 km-long fjord-shelf-slope transect, Kangerlussuaq margin, East Greenland. *Quaternary Science Reviews*, *29*(25-26), 3359–3369.

Dyke, L. M., Hughes, A. L. C., Andresen, C. S., Murray, T., Hiemstra, J. F., Bjørk, A. A., & Rodés, Á. (2018). The deglaciation of coastal areas of southeast Greenland. *The Holocene*, *28*(9), 1535–1544.

Fenty, I., Willis, J., Khazendar, A., Dinardo, S., Forsberg, R., Fukumori, I., et al. (2016). Oceans melting Greenland: Early results from NASA's ocean-ice mission in Greenland. *Oceanography*, *29*(4), 72–83.

Holland, D. M., Thomas, R. H., de Young, B., Ribergaard, M. H., & Lyberth, B. (2008). Acceleration of Jakobshavn Isbræ triggered by warm subsurface ocean waters. *Nature Geoscience*, *1*(10), 659–664.

Howat, I. M., Ahn, Y., Joughin, I., Van Den Broeke, M. R., Lenaerts, JanTM, & Smith, B.(2011). Mass balance of Greenland's three largest outlet glaciers, 2000-2010. *Geophysical Research Letters*, *38*, L12501. https://doi.org/10.1029/2011GL047565

Howat, I. M., & Eddy, A. (2011). Multi-decadal retreat of Greenland's marine-terminating glaciers. *Journal of Glaciology*, *57*(203), 389–396.

Howat, I. M., Joughin, I., Tulaczyk, S., & Gogineni, S. (2005). Rapid retreat and acceleration of Helheim Glacier, east Greenland. *Geophysical Research Letters*, *32*, L22502. https://doi.org/10.1029/2005GL024737

Howat, I. M., Smith, B. E., Joughin, I., & Scambos, T. A. (2008). Rates of southeast Greenland ice volume loss from combined ICESat and ASTER observations. *Geophysical Research Letters*, *35*, L17505. https://doi.org/10.1029/2008GL034496

Jakobsson, M., Mayer, L., Coakley, B., Dowdeswell, J. A., Forbes, S., Fridman, B., et al. (2012). The International Bathymetric Chart of the Arctic Ocean (IBCAO) version 3.0. *Geophysical Research Letters*, *39*, L12609. https://doi.org/10.1029/2012GL052219

Jennings, A. E., Hald, M., Smith, M., & Andrews, J. T. (2006). Freshwater forcing from the Greenland Ice Sheet during the Younger Dryas: Evidence from southeastern Greenland shelf cores. *Quaternary Science Reviews*, *25*(3-4), 282–298.

Millan, R., Rignot, E., Mouginot, J., Wood, M., Bjørk, A. A., & Morlighem, M. (2018). Vulnerability of southeast Greenland glaciers to warm Atlantic water from operation IceBridge and ocean melting Greenland data. *Geophysical Research Letters*, *45*, 2688–2696. https://doi.org/10.1002/2017GL076561

Morlighem, M., Williams, C. N., Rignot, E., An, L., Arndt, J. E., Bamber, J. L., et al. (2017). BedMachine v3: Complete bed topography and ocean bathymetry mapping of Greenland from Multibeam echo sounding combined with mass conservation. *Geophysical Research Letters*, *44*, 11,051–11,061. https://doi.org/10.1002/2017GL074954

Mouginot, J., Rignot, E., Bjørk, A. A., van den Broeke, M., Millan, R., Morlighem, M., et al. (2019). Forty-six years of Greenland Ice Sheet mass balance from 1972 to 2018. *Proceedings of the National Academy of Sciences*, *116*(19), 9239–9244. https://doi.org/10.1073/pnas.1904242116

Murray, T., Scharrer, K., James, T. D., Dye, S. R., Hanna, E., Booth, A. D., et al. (2010). Ocean regulation hypothesis for glacier dynamics in southeast Greenland and implications for ice sheet mass changes. *Journal of Geophysical Research*, *115*, F03026. https://doi.org/10.1029/2009JF001522

Parker, R. (1972). The rapid calculation of potential anomalies. *Geosciences Journal*, *31*(4), 447–455.

Porter, D. F., Tinto, K. J., Boghosian, A., Cochran, J. R., Bell, R. E., Manizade, S. S., & Sonntag, J. G. (2014). Bathymetric control of tidewater glacier mass loss in northwest Greenland. *Earth and Planetary Science Letters*, *401*, 40–46.

Rignot, E., Xu, Y., Menemenlis, D., Mouginot, J., Scheuchl, B., Li, X., et al. (2016). Modeling of ocean-induced ice melt rates of five west Greenland glaciers over the past two decades. *Geophysical Research Letters*, *43*, 6374–6382. https://doi.org/10.1002/2016GL068784

Smith, W. H. F., & Wessel, P. (1990). Gridding with continuous curvature splines in tension. *Geophysics*, *55*, 293–305. https://doi.org/10.1190/1.1442837

Straneo, F., Sutherland, D. A., Holland, D., Gladish, C., Hamilton, G. S., Johnson, H. L., et al. (2012). Characteristics of ocean waters reaching Greenland's glaciers. *Annals of Glaciology*, *53*(60), 202–210.

Wood, M., Rignot, E., Fenty, I., Menemenlis, D., Millan, R., Morlighem, M., et al. (2018). Ocean-induced melt triggers glacier retreat in Northwest Greenland. *Geophysical Research Letters*, *45*, 8334–8342. https://doi.org/10.1029/2018GL078024